ISSN: 2641-2039
DOI: 10.33552/GJES.2022.10.000743
Global Journal of Engineering Sciences
Iris Publishers

Research Article

The Effectiveness of using Advanced Optimization Algorithms in Heat Exchanger Design

AA Mohamed, Osama Mohammed Elmardi SK*, FA Elmahi, MV Fahmi and MA Mansour

Department of Mechanical Engineering, Faculty of Engineering and Technology, Nile Valley University, Atbara, Sudan

***Corresponding author:** Osama Mohammed Elmardi Suleiman Khayal, Department of Mechanical Engineering, Faculty of Engineering and Technology, Nile Valley University, Atbara, Sudan.

Received Date: November 25, 2022

Published Date: December 13, 2022

Abstract

Nowadays, using advanced optimization algorithms has become very popular in engineering design due to different factors among them are the time and effort high reduction to reach the optimum configuration. In the current research paper, comprehensive thermohydraulic modeling of fins and tube heat exchangers are conducted. This work examines the implementation and superiority of recently invented optimization algorithms in optimizing the particular heat exchangers under study. The algorithms used in the present work are Sine Cosine Algorithm SCA, JAYA Algorithm, and Grey Wolf Optimizer GWO. Three different population sizes, 25, 50, and 100 are used to ensure the judgment of performance superiority. The objective function of this study is to minimize the annual cost and maximize the effectiveness of heat exchangers. The results show that the best algorithm in optimizing the fins and tube heat exchanger over the three examined algorithms is Grey Wolf Optimizer GWO.

Keywords: Metaheuristics algorithms; Optimal design; Heat exchangers; Effectiveness; Cost

Introduction

With the rising heat dissipation demand, heat exchangers play a vital role in industrial and engineering applications as a device to achieve that objective. Fins and tube heat exchangers (FTHE) are considered as a class of compact heat exchangers. To classify the heat exchanger as compact, it must obtain a surface area density above 500 m^2/m^3 or a hydraulic diameter $D_h \leq 6mm$ [1-3]. In general, designing a FTHE is a complex mission since it needs comprehensive and integrated knowledge of fluid mechanics and heat transfer. The FTHE design process is iterative since it depends on a trial and error method to satisfy particular requirements related to the operational and configurational aspects [4]. The invention of metaheuristic algorithms and their implementation in designing and optimizing heat exchangers makes the process easier and having higher accuracy [5].

Several researchers used various optimization algorithms with different approaches and objective functions in the literature to optimize FTHEs. To predict the heat transfer characteristics of FTHE, Pacheco-Vega et al. [6] and [7] performed several tests and collected data. The researchers used regression analysis to determine the relationship between heat transfer characteristics and numerical data, which was subsequently, optimized using Genetic Algorithms (GA) and Simulated Annealing (SA). In place of the conventional trial-and-error approach, Xie et al. [8] applied a genetic algorithm (GA) to the thermal design of FTHE. In their study, the authors considered the minimum annual cost and minimum total weight as objective functions. Wu et al. [9] optimized the domestic refrigerator's optimum design parameters values under frosting conditions to enhance thermal performance, utilizing Taguchi techniques and response surface, the authors optimized the operation's average heat transfer rate, frost mass, and duration. FTHE optimization to minimize tube length and maximize the heat transfer rate in refrigerant circuits was performed by Wu et al. [9] using GA. A novel approach to identifying the optimal configuration of FTHE used in air conditioning applications has been proposed by Saechan et al. [10]. The model presented in their research paper was based on the second law of thermodynamics to optimize entropy generation. Tang et al. [11] performed a thermal optimization using GA of the airside of FTHE. In this work, numerous fin patterns are used to correlate a relationship between thermal and hydraulic behavior, which is improved later by using GA. H. Hajabdollahi [12] conducted extensive thermohydraulic modeling of FTHE to identify optimum design parameter values using a nondominated sorting genetic algorithm (NSGA-II). In this work, the authors attempted

to identify the effect variation of each design parameter on the objective function results. By implementing the heat transfer search (HTS) optimization Algorithm, Raja et al. [13] optimized FTHE considering the heat exchanger's minimum total weight and cost as an objective function for the optimization. The observation from the above previous literature is that the majority of optimization algorithms used in the optimization of fin and tube heat exchangers have belonged to the classical class of optimization algorithms, and there is a clear gap in the implementation of recently invented optimization algorithms. Moreover, there is an actual need to show the superiority of some advanced optimization algorithms over other different algorithms in designing and optimizing FTHE.

The contributions of this work can be summarized as follows:

To examine and assess the superiority of three newly invented advanced optimization algorithms: the Sine Cosine Algorithm (SCA), the Jaya Algorithm, and the Grey Wolf Optimizer (GWO) for thermohydraulic modeling and design optimization of a fin-and-tube heat exchanger.

In contrast to the previous works, in this paper authors used three different population size values (25, 50 and 100) instead of just one value to identify the superiority and domination of a particular algorithm over the algorithms mentioned above.

Thermohydraulic Model Formulation

Figure 1 below illustrates a typical three-dimensional model of a fin and tube heat exchanger with plain fins.

Use subscripts 1 and 2 to denote the tube outside and inside, respectively. The geometrical characteristics are as follows:

For the tube outside surface

Figure 2 below shows the Schematic of the fin and Tube Heat exchanger and its terminology.

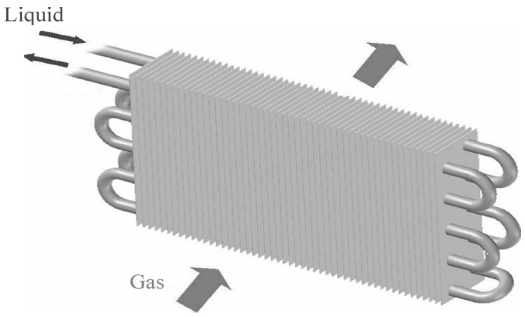

Figure 1: Three-Dimensional Model of Fin and Tube Heat Exchanger.

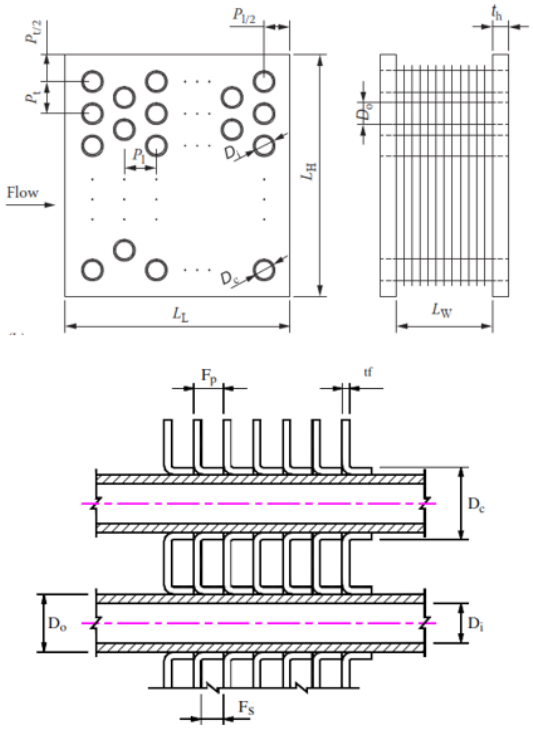

Figure 2: Schematic Representation of the Fin and Tube Heat Exchanger and its Terminology.

In Figure 2, L_L, L_W, and L_H denote the heat exchanger length, width, and height, respectively. D_o and D_i represent the outer and inner diameters of the tubes, whereas D_c is the collar diameter. P_t and P_l are the transverse and longitudinal pitch. t_f is the fin thickness, whereas t_h is the header thickness. F_p and F_s represent the fin pitch and fin spacing.

To determine the number of tubes, the following formula is used [1] as shown in Equation (1) below:

$$N_t = \left(\frac{L_H}{P_t}\right)\left(\frac{(L_L/P_l)+1}{2}\right)+\left(\frac{L_H}{P_t}-1\right)\left(\frac{(L_L/P_l)-1}{2}\right) \quad (1)$$

The number of fins is determined as represented in Equation (2) below:

$$N_f = \left(\frac{L_W}{F_P}\right)+1 \quad (2)$$

The total surface area of the tube outside surface is a combination of primary (tubes) A_p and secondary (fins) A_f areas and is calculated as follows (as presented in Equations (3), (4) and (5) below):

$$\mathrm{A_l = A_P + A_f} \quad (3)$$

$$\mathrm{A_P} = \pi D_c\left(L_W - \mathrm{t_f N_f} L_W\right)\mathrm{N}_t + 2\left(L_L L_H - 0.25\pi D_c^2 \mathrm{N}_t\right) \quad (4)$$

$$A_f = 2\left(L_L L_H - 0.25\pi D_c^2 \mathrm{N}_t\right) N_f L_W + 2\left(L_H \mathrm{t_f N_f} L_W\right) \quad (5)$$

The number of tubes rows is computed as in Equation (6) below:

$$\mathrm{N}_r = \frac{L_L}{P_l} \quad (6)$$

The minimum free flow area for the staggered arrangement is presented as shown in Equation (7) below:

$$\mathrm{A}_{o1} = \left(\left(\frac{L_H}{P_t}-1\right)c + \left(P_t - D_c\right) - \left(P_t - D_o\right)\mathrm{t_f N_f}\right) L_W \quad (7)$$

The core frontal area is calculated as follows (Equation (8) below):

$$\mathrm{A}_{fr1} = L_W L_H \quad (8)$$

The ratio of the free flow area to the frontal area, σ is as clarified in Equation (9) below:

$$\sigma_1 = \frac{\mathrm{A}_{o1}}{\mathrm{A}_{fr1}} \quad (9)$$

The hydraulic diameter of the tube outside is formulated in Equation (10) below:

$$\mathrm{D}_{h1} = \frac{4\mathrm{A}_{o1} L_L}{A_1} \quad (10)$$

The heat exchanger total volume is calculated using Equation (11) below:

$$\mathrm{V}_{tot} = L_W L_L L_H \quad (11)$$

The surface area density, α_1 is computed using Equation (12) below:

$$\alpha_1 = \frac{\mathrm{A}_1}{\mathrm{V}_{tot}} \quad (12)$$

For the tube inside surface (liquid side)

The total heat transfer area is calculated as shown in Equation (13) below:

$$\mathrm{A}_2 = \pi D_i L_W N_t \quad (13)$$

The minimum free flow area is calculated using the formula shown below (Equation (14)):

$$\mathrm{A}_{o2} = 0.25\pi D_i^2 \mathrm{N}_t \quad (14)$$

The core frontal area is determined as shown below (Equation (15)):

$$\mathrm{A}_{fr2} = L_L L_H \quad (15)$$

The ratio of the free flow area to the frontal area, σ is determined using the following formula (Equation (16) below):

$$\sigma_2 = \frac{\mathrm{A}_{o2}}{\mathrm{A}_{fr2}} \quad (16)$$

The surface area density, α_2 is computed using Equation (17) below:

$$\alpha_2 = \frac{\mathrm{A}_2}{\mathrm{V}_{tot}} \quad (17)$$

The hydraulic diameter of the tube outside is formulated in Equation (18) below:

$$\mathrm{D}_{h2} = D_i \quad (18)$$

Heat transfer coefficients

For the tube outside (airside), when the tube rows are equal to or greater than two (N≥2), then the Colburn factor (j_a) is calculated from the correlation of Wang et al. [14] as follows (Equations (19 – 24) below):

$$j_1 = -0.361 - \frac{0.042 N_r}{\ln(\mathrm{Re}_{D_c})} + 0.158\ln\left(N_r\left(\frac{F_P}{D_c}\right)^{0.41}\right) \quad (19)$$

$$j_2 = -1.224 - \frac{0.076\left(\frac{P_l}{D_{h_1}}\right)^{1.42}}{\ln(\mathrm{Re}_{D_c})} \quad (20)$$

$$j_3 = -0.083 + \frac{0.058 N_r}{\ln(\mathrm{Re}_{D_c})} \quad (21)$$

$$j_4 = -5.735 + 1.21 \ln\left(\frac{\mathrm{Re}_{D_c}}{N_r}\right) \qquad (22)$$

Where: Re_{D_c} Represents Reynold's number calculated based on collar diameter.

The Colburn factor (j_a) is calculated using Equation (23) below:

$$j_\alpha = 0.086(\mathrm{Re}_{D_c})^{j_1} (N_r)^{j_2} \left(\frac{F_P}{D_c}\right)^{j_3} \left(\frac{F_P}{D_{h1}}\right)^{j_4} \left(\frac{F_P}{P_t}\right)^{-0.93} \qquad (23)$$

After that, the heat transfer coefficient on the tube outside (h_a) is calculated as follows (Equation (24)):

$$\mathrm{h}_a = j_a \left(\frac{4\rho_a V_a c_{pa}}{P_a^{0.67}}\right) \qquad (24)$$

Where: V_a, C_{pa}, ρ_a, and P_{ra} represent the velocity, specific heat, density, and Prandtl number.

For the tube inside (waterside) to determine the Nusselt number (Nu_w) Gnielinsk correlation is used; this correlation is stated as shown in Equation (25) below:

$$\mathrm{Nu}_w = \frac{\left(\frac{f_w}{2}\right)(\mathrm{Re}_w - 1000)\,\mathrm{P}r_w}{1 + 12.7\left(\frac{fw}{2}\right)^{1/2}\left(\mathrm{P}r_w^{2/3} - 1\right)} \qquad (25)$$

Here, Pr_w and Re_w denote Prandtl number and Reynolds number, respectively. f_w represents the friction factor which can be calculated as mentioned in Equation (26) below:

$$f_w = \left(1.82 \log_{10} \mathrm{Re}_w - 1.64\right)^{-2} \qquad (26)$$

Then calculate the heat transfer coefficient on the waterside (h_w) is determined by using Equation (27) below:

$$h_w = \frac{\mathrm{Nu}_w k_w}{D_i} \qquad (27)$$

Where: k_w represents the thermal conductivity of water.

Pressure drop

The friction factor on the airside (f_a) is calculated based on Wang et al. [14] correlation as explained in Equation (28) below:

$$\mathrm{f}_a = 0.0267\left(\mathrm{Re}_{D_c}\right)^{f_1} \left(\frac{P_t}{P_l}\right)^{f_2} \left(\frac{F_P}{D_c}\right)^{f_3} \qquad (28)$$

Where: f_1, f_2 and f_3 denote different coefficients, and their mathematical details are formulated as follows (Equations (29) – (31)):

$$\mathrm{f}_1 = -0.764 + 0.739\left(\frac{P_t}{P_l}\right) + 0.177\left(\frac{F_P}{D_c}\right) - \frac{0.00758}{N_r} \qquad (29)$$

$$\mathrm{f}_2 = -15.689 + \frac{64.021}{\ln\left(\mathrm{Re}_{D_c}\right)} \qquad (30)$$

$$\mathrm{f}_3 = 1.696 - \frac{15.695}{\ln\left(\mathrm{Re}_{D_c}\right)} \qquad (31)$$

For airside, the pressure is calculated as shown in Equation (32) below:

$$\Delta \mathrm{P}_a = \frac{G_a^2}{2\rho_{a,i}}\left[\frac{A_1}{A_{o1}}\frac{\rho_{a,i}}{\rho_{a,m}} f_a + \left(1 + \sigma_1^2\right)\left(\frac{\rho_{a,i}}{\rho_{a,o}} - 1\right)\right] \qquad (32)$$

Where: $\rho_{(a,i)}$, $\rho_{(a,o)}$, and $\rho_{(a,m)}$ denote the inlet, outlet, and mean density of air, whereas G_a represents the mass velocity of the air.

For waterside, the pressure is calculated as shown in Equation (33) below:

$$\Delta \mathrm{P}_w = \frac{f_w \rho_w V_w^2 (L_W + 2t_h)}{2D_i} \qquad (33)$$

Where: V_w denotes water velocity and ρ_w represents water density.

Overall heat transfer coefficient

The overall heat transfer coefficient is determined as shown in Equation (34) below:

$$U_o = \frac{1}{\left(\frac{1}{h_a}\right) + \left(\frac{A_1}{A_2 h_w}\right)} \qquad (34)$$

Optimization

This section summarizes the multi-objective optimization problems such as concept, advanced optimization algorithms used to conduct this paper, design variables, objective function, and constraints applied through this design optimization process.

Multi-Objective optimization problems

Optimization means finding one or more of the possible solutions associated with the extreme (i.e. minimum or maximum) values of one or more particular objectives [15]. In general, multi-objective optimization problems (MOOP) have several conflicting objective functions, which may be equal to, or more than two objective functions. The MOOP could be expressed mathematically based on [16] as explained in Equations (35) – (38):

$$Min / Max\ f_m(X), \qquad m=1,2,...,M \qquad (35)$$

$$Subject\ to\ g_j(X) \le 0, \qquad j=1,2,...,J \qquad (36)$$

$$h_k(X) = 0, \qquad k=1,2,...,K \qquad (37)$$

$$x_i^{(L)} \le x_i \le x_i^{(U)}, \qquad i=1,2,...,n \qquad (38)$$

Where solution X represents the vector of design variables $X=(x_1,x_2,...,x_n)$ whereas $x_i^{(L)}$ and $x_i^{(U)}$ denote lower bounds (LB) and upper bounds (UB), respectively. The terms g_j, h_k represent inequality and equality constraints. One of the popular methods to deal with multi-objective optimization is the Epsilon Constraint method. In this method, one of the objective functions is considered a primary objective function, and the remaining functions are considered a secondary objective function and converted to constraints. In the current research paper, multi-objective optimization is performed based on the Epsilon Constraint method.

Advanced optimization algorithms

Population-based optimization techniques generally start the optimization process with a set of random solutions. This random set is evaluated repeatedly by an objective function and improved by a group of rules that is the core of an optimization technique. Usually, the significant difference between the Population-based algorithms confines two factors, their specific parameters and the equations proposed for position updating. This section describes the two factors for the different algorithms used in the present work.

Sine Cosine Algorithm (SCA): SCA is one of the population-based algorithms invented by Seyedali Mirjalili in 2016 [17]. The author proposed the following equation (Equation (39)) for position updating.

$$X_i^{t+1} = \begin{cases} X_i^t + r_1 \times \sin(r_2) \times \left| r_3 P_i^t - X_i^t \right|, & r_4 < 0.5 \\ X_i^t + r_1 \times \cos(r_2) \times \left| r_3 P_i^t - X_i^t \right|, & r_4 \ge 0.5 \end{cases} \qquad (39)$$

Where X_i^t is represents the current solution position at the i^{th} dimension and the t^{th} iteration. P_i^t Represents the destination position. The r_1, r_2 and r_3 denote random numbers. The r_4 random number in [0, 1].

JAYA Algorithm: Jaya is another class of population-based optimization algorithm invented in 2016 by R. Venkata Rao [18]. This work suggests **EQ.25115** for updating the position as shown in Equation (40) below.

$$X_i^{t+1} = X_i^t + r_1 \left(X_{Best} - \left| X_i^t \right| \right) - r_2 \left(X_{Worst} - \left| X_i^t \right| \right) \qquad (40)$$

Where X_{Best} and X_{Worst} are the best and worst candidate solutions, respectively. The r_1 and r_2 represent random numbers in a range [0, 1] as before.

Grey Wolf Optimizer (GWO): GWO is the last optimization algorithm used in this research paper and is another class of population-based algorithms. In 2014, Seyedali Mirjalili et al. [19] created a new optimization algorithm based on social hierarchy and the hunting behavior of grey wolves. In that work, the authors proposed the following equations (Equations (41) – (54)) for position updating.

$$X_i^{t+1} = \frac{X_1 + X_2 + X_3}{3} \qquad (41)$$

$$X_1 = X_\alpha - A_1 D_\alpha \qquad (42)$$

$$D_\alpha = \left| C_1 X_\alpha - X_i^t \right| \qquad (43)$$

$$C_1 = 2rand \qquad (44)$$

$$A_1 = 2a.rand - a \qquad (45)$$

$$X_2 = X_\beta - A_2 D_\beta \qquad (46)$$

$$D_\beta = \left| C_2 X_\beta - X_i^t \right| \qquad (47)$$

$$C_2 = 2rand \qquad (48)$$

$$A_2 = 2a.rand - a \qquad (49)$$

$$X_3 = X_\delta - A_3 D_\delta \qquad (50)$$

$$D_\delta = \left| C_3 X_\delta - X_i^t \right| \qquad (51)$$

$$C_3 = 2rand \qquad (52)$$

$$A_3 = 2a.rand - a \qquad (53)$$

$$a = 2\left(1 - \frac{iteration}{max\ iteration} \right) \qquad (54)$$

Where: X_α, X_β, and X_δ denote the best position, the second-best position, and the third best position over the candidate solution. The rand is the random number between 0 and 1.

Design variables

In this research paper, seven parameters have been considered as design variables which are the longitudinal pitch P_l, transverse pitch P_t, fin pitch F_p, outer tube diameter D_o, the length of the cold flow path (width dimension) L_W, the length of the no-flow path (height dimension) L_H, and the fin thickness t_f. Table 1 below summarizes the design variables considered in this work and their

ranges. For simplification, the value of the tube's inner diameter was taken equivalent to 0.8 of the outer diameters.

Objective function

In the present work, the minimum annual cost (C_{tot}) and maximum effectiveness (ε) were considered bi-objective functions. The minimum yearly cost consists of two components, initial cost (C_{in}) and operating cost (C_{op}).

$$C_{tot} = C_{in} + C_{op} \qquad (55)$$

Table 1: Design Variables and their Ranges.

Design Variables	Lower Bounds	Upper Bounds
P_l, mm	12.7	32
P_t, mm	20.4	31.8
F_p, mm	1	8.7
D_O, mm	6.8	12.7
L_W, mm	200	1000
L_H, mm	200	1000
t_f, mm	0.1	0.33

$$C_{in} = C_A A_1^n \qquad (56)$$

$$C_{op} = \left(\frac{k_{el}\tau\Delta P_a V_{t,a}}{\eta}\right) + \left(\frac{k_{el}\tau\Delta P_w V_{t,w}}{\eta}\right) \qquad (57)$$

C_A denote the cost per unit surface area, k_{el} is the electricity price, V_t the volumetric flow rate, τ is the operation hours, η represents the efficiency of the pump/compressor.

The effectiveness of a fin-and-tube heat exchanger (crossflow heat exchanger with both fluids unmixed) based on [4] as in Equation (58) below.

$$\varepsilon = 1 - \exp\left(\frac{NTU^{0.22}}{C}\left(\exp\left(-C * NTU^{0.78}\right) - 1\right)\right) \qquad (58)$$

The number of transfer units (NTU) and heat capacity ratio C are defined as follows (as shown in Equations (59) and (60) below):

$$\mathrm{NTU} = \frac{U_o A_1}{C_{\min}} \qquad (59)$$

$$C = \frac{C_{\min}}{C_{\max}} = \frac{\left(\dot{m} C_p\right)_{\min}}{\left(\dot{m} C_p\right)_{\max}} \qquad (60)$$

Constraints applied

The above-mentioned bi-objective functions had subjected to the following set of constraints as explained in Equations (61) – (78) below:

$$g_1(X): \Delta P_a - \Delta P_{a,\max} \le 0 \qquad (61)$$

$$g_2(X): \Delta P_w - \Delta P_{w,\max} \le 0 \qquad (62)$$

$\Delta P_{(a,max)}$, $\Delta P_{(w,max)}$ Denotes the maximum allowable pressure drop. In the present work, the maximum allowable pressure drop is set as 3% of entrance pressure for each side; based on that, the values of $\Delta P_{(a,max)}$, $\Delta P_{(w,max)}$ are 7.5 kN/m^2, and 6 kN/m^2 respectively.

$$g_3(X): 60 - \frac{L_W}{D_o} \le 0 \qquad (63)$$

$$g_4(X): \mathrm{Re}_{D_c} - 20000 \le 0 \qquad (64)$$

$$g_5(X): 300 - \mathrm{Re}_{D_c} \le 0 \qquad (65)$$

$$g_6(X): \mathrm{Re}_w - 2\times 10^6 \le 0 \qquad (66)$$

$$g_7(X): 2300 - \mathrm{Re}_w \le 0 \qquad (67)$$

The validity of Equation (32) based on [14] is within the range of $300 \le \mathrm{Re}_{D_c} \le 2000$, $6.9\mathrm{mm} \le D_c \le 13.6\mathrm{mm}$, $20.4\mathrm{mm} \le P_t \le 31.8\mathrm{mm}$, $12.7\mathrm{mm} \le P_l \le 32\mathrm{mm}$, and $1\mathrm{mm} \le F_p \le 8.7\mathrm{mm}$, so it is very convenient to apply that validity ranges to the mentioned objective function.

$$g_8(X): 6.9 - D_c \le 0 \qquad (68)$$

$$g_9(X): D_c - 13.6 \le 0 \qquad (69)$$

$$g_{10}(X): 20.4 - P_t \le 0 \qquad (70)$$

$$g_{11}(X): P_t - 31.8 \le 0 \qquad (71)$$

$$g_{12}(X): 12.7 - P_t \le 0 \qquad (72)$$

$$g_{13}(X): P_l - 32 \le 0 \qquad (73)$$

$$g_{14}(X): 1 - F_P \le 0 \qquad (74)$$

$$g_{15}(X): F_P - 8.7 \le 0 \qquad (75)$$

$$g_{16}(X): 1 - \frac{A_1}{A_f} \le 0 \qquad (76)$$

$$g_{17}(X): \frac{A_1}{A_f} - 1.2 \le 0 \qquad (77)$$

According to [12], the practical effectiveness range of FTHE varies from 0.5 to 0.78 (0.5<ε<0.78), so the maximum possible practical effectiveness (ε_{max}) set to 0.78.

$$g_{18}(X): \frac{A_1}{A_f} - 1.2 \le 0 \qquad (78)$$

Case Study

Case study data

This section summarizes the case study used to illustrate how to use the above-formulated thermohydraulic model. The data used in this case study were according to references [4], and [12].

Table 2 shows the operating conditions (process input and economics parameters) used in the present work. The properties of water and air, such as density, viscosity, specific heat, and Prandtl number, had been considered temperature-dependent. Their values were collected from G. Rogers and Y. Mayhew's thermophysical properties tables [20].

Table 2: Case Study Data from References [4,12].

Operating Conditions	Air	Water
$\dot{m}$, Kg/s	2.5	3.2
T_i, °C	152	12
T_o, °C	40	-
P_i, kPa	250	200
K_{el}, $/MWh	25	25
n	0.6	-
τ, h/year	5000	5000
η	0.65	0.65
C_A, $/m^2	85	-

Results and Discussion

In the current work, the design optimization of FTHE was performed using three different recently invented advanced optimization algorithms (SCA, JAYA, and GWO). The modeling was conducted using three different population sizes (P=25, P=50, and P=100). Each algorithm runs 21 times to find the optimum solution, maximizing effectiveness and minimizing total cost. The abbreviation R21P25, R21P50, and R21P100 denotes the cases, where R means the number of runs and P means population sizes used. The termination criteria of the modeling set as 5000 iterations applied in each run through all cases.

Before diving into basic statistics for each algorithm, firstly Friedman test (F-test) must be performed to identify whether there is an actual difference between the algorithms mentioned above. Friedman test is one of the most popular nonparametric tests used to compare the performance of metaheuristics optimization algorithms. The idea behind that is to consider two different hypotheses, H_o and H_1. The first hypothesis (H_o) is that there are no differences between the performance of the different algorithms; this hypothesis will be accepted if the calculated test statistic (T_2) is less than the tabulated one available in the F-test tables. The second hypothesis (H_1) is that there are differences between the performance of the different algorithms; this will be accepted if the calculated test statistic (T_2) is greater than the tabulated one available in the F-test tables. More details about F-test are available in [21]. The F-test conducted in the current research paper is performed using α=0.01, which means the reliability of the results is 0.99. Table 3 shows the comparison between the calculated test statistic and the tabulated one at $F_{(1-\alpha,k-1,(b-1)(k-1))}$, where k is the number of algorithms used during the comparison, and b is the number of runs, so the searching about tabulated value in the α=0.01 F-test tables will be at $F_{0.99,2,40}$. As shown in Table 3, the F-test shows that the calculated test statistic is greater than the tabulated one for all the cases R21P25, R21P50, and R21P100. Since T_2 is greater than $F_{0.99,2,40}$ that means the null hypothesis is rejected, and the H1 hypothesis is accepted. The results give a strong indication that for all cases, there is at least one algorithm that tends to perform better than the others do.

Table 4 presents the basic statistics of the results obtained by the different algorithms for the three cases.

Table 3: F-Test Statistic Comparison.

Case	T_2	$F_{0.99,2,40}$
R21P25	56.02	5.18
R21P50	9.2	5.18
R21P100	12.67	5.18

Table 4: Basic Statistics of the Results obtained by the Different Algorithms.

Case	Statistics	SCA	JAYA	GWO
R21P25	Best	320.8863	320.1549	320.012
	Worst	323.1969	402.4073	321.0708
	Mean	321.8746	334.8607	320.4479
	S.D.	0.6419	19.0423	0.3395
	Exec. time (sec)	74.8753	74.5397	114.6407
	No. of Succeeds	21	21	21
	No. of Failures	0	0	0
R21P50	Best	320.4974	319.8741	319.9346
	Worst	322.3431	462.9882	321.0254
	Mean	321.4068	335.1058	320.2696
	S.D.	0.4966	31.9165	0.3086
	Exec. time (sec)	79.5825	78.5527	189.7697
	No. of Succeeds	21	21	21
	No. of Failures	0	0	0
R21P100	Best	320.5393	319.8741	319.905
	Worst	321.7573	435.2783	321.0438
	Mean	321.2641	344.992	320.1732
	S.D.	0.3275	34.6879	0.2753
	Exec. time (sec)	85.0427	82.9627	453.669
	No. of Succeeds	21	21	21
	No. of Failures	0	0	0

In Table 4, the basic statistics are as follows: Best represents the best solution (minimum value of total cost), Worst is the worst solution (maximum value of total cost), Mean is the mean solution, S.D. represents the standard deviation of the mean solution, Exec. Time is the execution time, No. of succeed is the number of successful minimizations, and No. of Failure: number of failed minimizations. All these statistics are of 21 solutions obtained by SCA, JAYA, and GWO for the three cases, R21P25, R21P50, and R21P100.

Validation of the new generated results

Table 5: Comparison of Basic Geometrical Aspects for Case R21P25.

Geo. Aspects	Ref [4]	Ref [12]	Present Work					
			SCA	Diff. %	JAYA	Diff. %	GWO	Diff. %
D_o mm	10.2	-	10.06	-1.37	10.02	-1.76	10.16	-0.39
N_f	315	-	312	-0.95	317	0.63	317	0.63
D_h mm	3.632	3.368	3.132	-13.77	3.089	-14.95	3.08	-15.2
t_f mm	0.33	-	0.33	0	0.33	0	0.33	0
$\sigma 1$	0.534	0.495	0.433	-18.91	0.433	-18.91	0.43	-19.47
$\alpha 1$ m^2/m^3	587	587.76	554	-5.62	560	-4.6	559	-4.77
A_f/A_1	0.913	0.915	0.833	-8.76	0.833	-8.76	0.833	-8.76
Min. Cost	-	389.4	320.8863	-	320.1549	-	320.012	-
ε	-	0.7795	0.7802	-	0.78	-	0.7801	-
Mean absolute error (MAE)				7.05		7.09		7.03

Table 6: Comparison of Basic Geometrical Aspects for Case R21P50.

Geo. Aspects	Ref [4]	Ref [12]	Present Work					
			SCA	Diff. %	JAYA	Diff. %	GWO	Diff. %
D_0 mm	10.2	-	10.07	-1.27	10.21	0.1	10.17	-0.29
N_f	315	-	312	-0.95	315	0	318	0.95
D_h mm	3.632	3.368	3.13	-13.82	3.096	-14.76	3.072	-15.42
t_f mm	0.33	-	0.33	0	0.33	0	0.33	0
$\sigma 1$	0.534	0.495	0.433	-18.91	0.43	-19.48	0.43	-19.48
$\alpha 1$ m^2/m^3	587	587.76	554	-5.62	555	-5.45	559	-4.77
A_f/A_1	0.913	0.915	0.833	-8.76	0.833	-8.76	0.833	-8.76
Min. Cost	-	389.4	320.4974	-	319.8741	-	319.9346	-
ε	-	0.7795	0.7802	-	0.78	-	0.7805	-
Mean absolute error (MAE)				7.05		6.94		7.09

Table 7: Comparison of Basic Geometrical Aspects for Case R21P100.

Geo. Aspects	Ref [4]	Ref [12]	Present Work					
			SCA	Diff. %	JAYA	Diff. %	GWO	Diff. %
D_0 mm	10.2	-	10.27	0.69	10.21	0.1	10.25	0.49
N_f	315	-	314	-0.32	315	0	313	-0.63
D_h mm	3.632	3.368	3.106	-14.48	3.096	-14.76	3.112	-14.32
t_f mm	0.33	-	0.33	0	0.33	0	0.33	0
$\sigma 1$	0.534	0.495	0.429	-19.66	0.43	-19.48	0.43	-19.48
$\alpha 1$ m^2/m^3	587	587.76	553	-5.79	555	-5.45	552	-5.96
A_f/A_1	0.913	0.915	0.834	-8.65	0.833	-8.76	0.833	-8.76
Min. Cost	-	389.4	320.5393	-	319.8741	-	319.905	-
ε	-	0.7795	0.7803	-	0.78	-	0.7801	-
Mean absolute error (MAE)				7.08		6.94		7.09

In order to validate the design optimization results obtained from using the formulated model and the different algorithms, the design optimization results were compared with the reported data given in [3] and [11]. Tables 5, 6, and 7 compare the current work with references [4] and [12]. The comparisons are built on seven different geometrical characteristics (aspects), as shown in the tables. The individual differences of the compared aspects vary from 0% to 19.48%, whereas the mean absolute error (MAE) ranges between 6.94% and 7.09% for all cases through the different algorithms.

Figures 3, 4 and 5 represent the Box plot of the three cases over the different algorithms used.

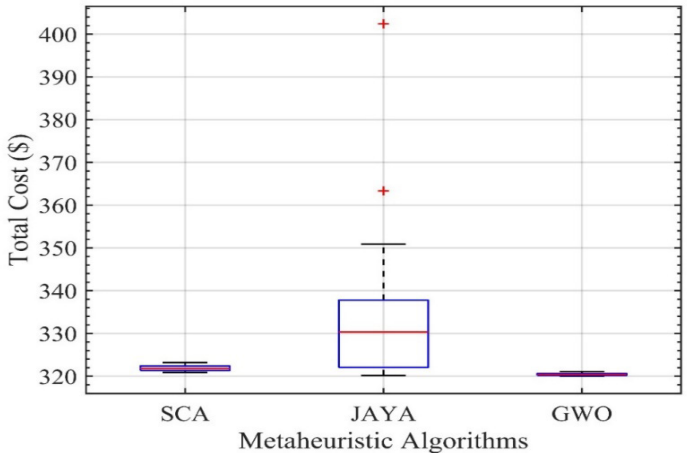

Figure 3: Box Plot of the Different Algorithms for Case R21P25.

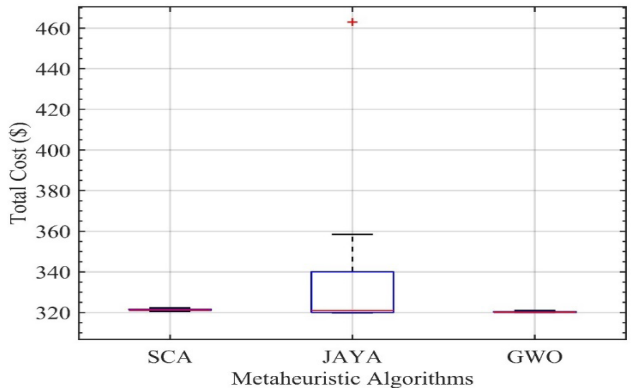

Figure 4: Box Plot of the Different Algorithms for Case R21P50.

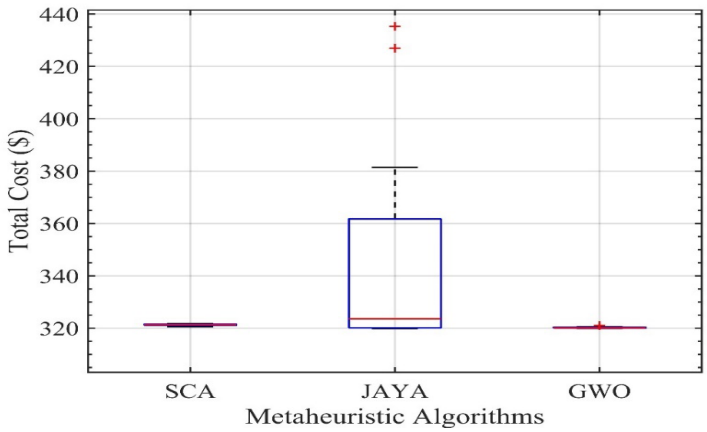

Figure 5: Box Plot of the Different Algorithms for Case R21P100.

Based on the data of Table 4 and the box plot of Figures 3, 4, and 5 can record several observations. Each of the statistics (median, upper quartile UQ, lower quartile LQ, and interquartile range IQR) for the GWO is lower than for SCA and JAYA through the three above-presented figures. Through all figures presented above GWO graph is slightly lower than SCA and JAYA graphs. Based on that, some evidence leads to the judgment that GWO performs better.

Figures 6, 7, and 8 show the effectiveness (ε) of the SCA, JAYA, and GWO for the optimized FTHE through the three cases. The maximum practical effectiveness (ε) for this class of compact heat exchangers is 78%. Based on these results, SCA, JAYA, and GWO show consistent behavior in maximizing FTHE effectiveness. Each of JAYA and GWO obtains effectiveness equal to that value almost in all cases. The SCA gives slightly higher values with differences ranging between 0.01 and 0.1 from the maximum practical effectiveness value.

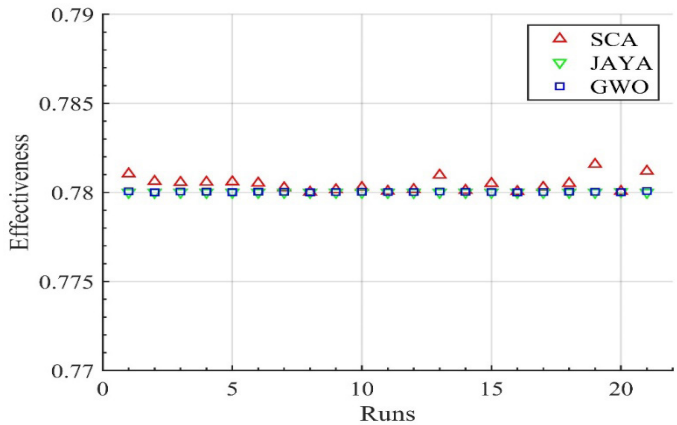

Figure 6: Effectiveness (ε) through the 21 Runs for Case R21P25.

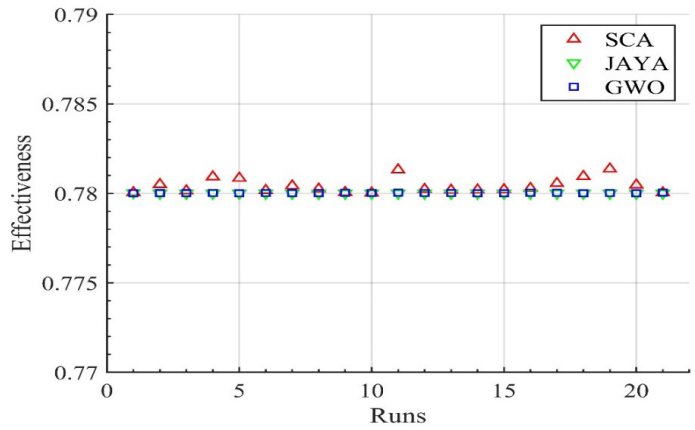

Figure 7: Effectiveness (ε) through the 21 Runs for Case R21P50.

Figure 9 presents the average ranks of each algorithm obtained from the F-test through the various cases. In general, through all compared cases, the GWO achieves the lowest average rank value providing evidence that GWO performs better than SCA and JAYA through all cases examined. In the case of R21P25, GWO achieved an average rank of 1.05, whereas SCA and JAYA obtained 2.24 and 2.71, respectively. In the case of R21P50, GWO achieved an average rank of 1.38, whereas SCA and JAYA received 2.48 and 2.14, respectively. In the case of R21P100, GWO achieved an average rank of 1.29, whereas SCA and JAYA obtained 2.43 and 2.29, respectively. Based on that, it is observed that when the population size is 25, SCA shows superiority compared to JAYA, but when the population size changes to 50 and 100, JAYA defeats SCA. According to the earlier remark, using various population size values to judge the algorithm's superiority is better.

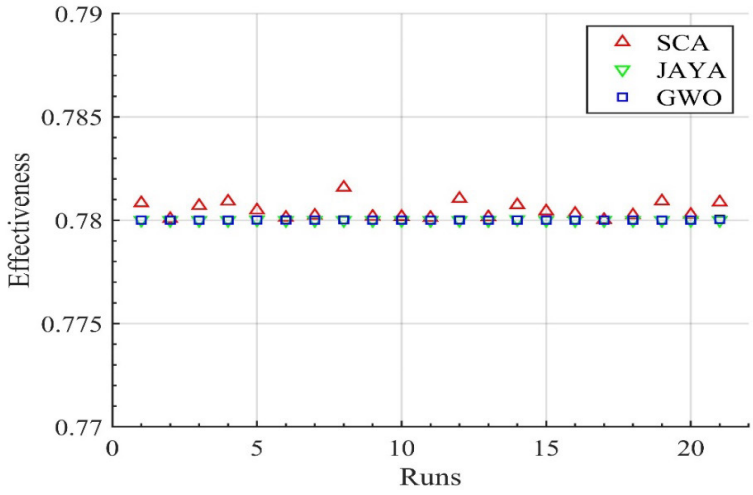

Figure 8: Effectiveness (ε) through the 21 Runs for Case R21P100.

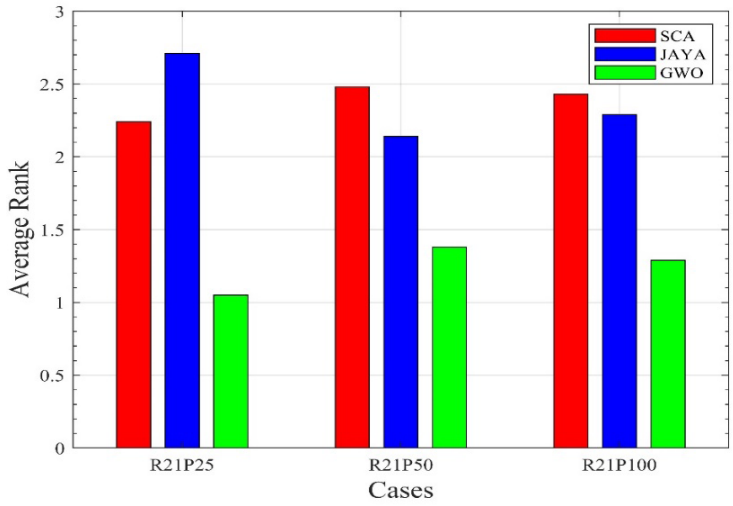

Figure 9: Average Rank of the Different Algorithms.

Conclusion

In the current work, a thermohydraulic model of fin and tube heat exchangers (FTHE) is fabricated from the basic knowledge of thermal engineering science and the correlations available in the literature. This mathematical model is used to find the optimal design (optimal configuration) of the FTHE. The design optimization of the FTHE performed in the present research paper was conducted using three different optimization algorithms: the sine cosine algorithm SCA, the JAYA algorithm, and the grey wolf optimizer GWO. Each algorithm is used to optimize the FTHE through various population sizes (P=25, P=50, and P=100) to judge the algorithm's superiority over each other. The GWO shows superior performance on SCA and JAYA through all the cases examined.

Acknowledgement

None.

Conflict of Interest

No conflict of interest.

References

1. Ramesh K Shah, Dusan P Sekulic (2003) Fundamentals of heat exchanger design. S.l., USA: WILEY-BLACKWELL.
2. Osama Mohammed Elmardi Suleiman Khayal (2018) Fundamentals of Heat Exchangers, International Journal of Research in Computer Applications and Robotics. 6(12): 1-11.
3. Osama Mohammed Elmardi (2017) Solutions to Problems in Heat Transfer. Transient Conduction or Unsteady Conduction, Publisher: Anchor Academic Publishing, pp. 108, ISBN-10: 3960671237, ISBN-13: 978-3960671237.
4. WM Kays, AL London (1998) Compact heat exchangers. Malabar, FL, USA: Krieger Pub. Co.
5. VK Patel, VJ Savsani, MA Tawhid (2019) Thermal system optimization: A population-based metaheuristic approach. Cham, Switzerland: Springer.
6. Arturo Pacheco-Vega, Sen M, Yang KT, McClain RL (2001) Correlations of fin-tube heat exchanger performance data using genetic algorithm, simulated annealing and interval methods. in In: Proceedings of ASME heat transfer division 369: 143-151.
7. A Pacheco-Vega, M Sen, KT Yang (2003) Simultaneous determination of in- and over-tube heat transfer correlations in heat exchangers by global regression. International Journal of Heat and Mass Transfer 46(6): 1029-1040.
8. G Xie, Q Wang, B Sunden (2008) Application of a genetic algorithm for thermal design of fin-and-tube heat exchangers. Heat Transfer Engineering 29(7): 597-607.
9. Z Wu, G Ding, K Wang, M Fukaya (2008) Application of a genetic algorithm to optimize the refrigerant circuit of fin-and-tube heat exchangers for maximum heat transfer or shortest tube. International Journal of Thermal Sciences 47(8): 985-997.
10. P Saechan, S Wongwises (2008) Optimal configuration of cross flow plate finned tube condenser based on the second law of Thermodynamics. International Journal of Thermal Sciences 47(11): 1473-1481.
11. LH Tang, M Zeng, QW Wang (2009) Experimental and numerical investigation on air-side performance of fin-and-tube heat exchangers with various fin patterns. Experimental Thermal and Fluid Science 33(5): 818-827.
12. H Hajabdollahi, P Ahmadi, I Dincer (2011) Multi-objective optimization of plain fin-and-tube heat exchanger using evolutionary algorithm. Journal of Thermophysics and Heat Transfer 25(3): 424-431.
13. BD Raja, V Patel, RL Jhala (2017) Thermal design and optimization of fin-and-tube heat exchanger using heat transfer search algorithm. Thermal Science and Engineering Progress 4: 45-57.
14. CC Wang, KY Chi, CJ Chang (2000) Heat transfer and friction characteristics of plain fin-and-tube heat exchangers, part II: Correlation. International Journal of Heat and Mass Transfer 43(15): 2693-2700.
15. D Kalyanmoy (2004) Optimization for Engineering Design: Algorithms and examples. New Delhi, India: Prentice-Hall of India Pvt. Ltd.
16. K Deb (2001) Multi-objective optimization using evolutionary algorithms. Chichester, England: John Wiley & Sons.
17. S Mirjalili (2016) SCA: A sine cosine algorithm for solving optimization problems. Knowledge-Based Systems 96: 120-133.

18. R Venkata Rao (2016) Jaya: A simple and new optimization algorithm for solving constrained and unconstrained optimization problems. International Journal of Industrial Engineering Computations, pp. 19-34.

19. S Mirjalili, SM Mirjalili, A Lewis (2014) Grey Wolf optimizer. Advances in Engineering Software 69: 46-61.

20. RGFC, YR Mayhew (1995) Thermodynamic and transport properties of fluids: SI units. B. Blackwell.

21. WJ Conover (1999) Practical nonparametric statistics. New York, USA: Wiley.